Indian Geotechnical Journal, 38(2), 2008, 119-139

A Fuzzy Meshless Method for Beams on Elastic Foundation

N. V. Sunitha[*], G. R. Dodagoudar[**] and B. N. Rao[***]

Introduction

Mainly there are two basic types of elastic foundations. The first type is furnished by the elastic solid, which represents the case of complete continuity in the supporting medium. This type of elastic support can be provided in the form of a load-bearing medium such as soil, distributed continuously along the length of the beam. The second type is characterized by the fact that the pressure on the foundation is proportional at every point to the deflection occurring at that point and is independent of deflections produced elsewhere in the foundation which is in contrast with the first type. Second type of supports can be found in a variety of engineering problems, for example in the case of actual foundations or in the case of railroad track. Apart from the diversity of technical applications, there is a considerable variation possible in the fundamental aspects of this approach. The flexural rigidity of the beam or the elasticity of the foundation may be a variable quantity; the axis of the beam may be straight or curved or the character of the applied loading may be axial, transverse, or torsional, in addition to a combination of end conditions to which any of these beams may be subjected. All these problems are closely related in their mathematical formulation (Hetenyi 1958). A primary difficulty in the analysis of soil foundation interaction lies in the determination of the contact pressure. Strictly speaking any of the constitutive models may be used for simulating the action of the soil media. Some models are so complicated that they find limited practical applications (Cheung and Tham 1993).

Meshfree (meshless) methods have become attractive alternatives for problems in computational solid mechanics, as they do not require a mesh to discretize the problem domain. The approximate solution is constructed entirely in terms of a set of scattered nodes. In the traditional meshless analysis, system parameters such as mass, geometry and material properties are assumed to be known precisely and defined in exact terms. When such design model contains uncertain physical properties for which no objective statistical data is available, a probabilistic analysis leads to subjective and misleading conclusions, and it is therefore not reliable for objective design validation purposes. An alternative method to describe these uncertainties is provided by the concept of fuzzy numbers, which has led to the development of Fuzzy Meshless Method. The

* Research Scholar, Dept. of Civil Engineering, I.I.T. Madras, Chennai - 600 036. Email: suni_nv@yahoo.com

** Asst. Professor, Dept. of Civil Engineering, I.I.T. Madras, Chennai - 600 036. Email: goudar@iitm.ac.in

*** Asst. Professor, Dept. of Civil Engineering, I.I.T. Madras, Chennai - 600 036. Email: bnrao@iitm.ac.in

meshless method is a new concept which can be used to overcome difficulties of the finite element method used for analyzing soil-structure interaction problems. The use of a mesh (be it domain or boundary one) is a basic characteristic of the traditional approaches for the solution of partial differential equations. Recent developments using the Element Free Galerkin Method (EFGM) as a meshless computational method for solving various kinds of partial and integral equations have been quite successful (Liu 2003). It has been proposed in this paper to use EFGM, which is simple but sufficiently accurate model for beams on elastic foundations (Sunitha 2007).

In the present paper, a beginning has been made to explore the possibility of using meshless techniques for analysing beams on elastic foundations considering uncertain variables such as subgrade modulus and applied load. A meshless formulation using EFGM is provided for the governing equation of the beams on elastic foundation, in which the soil medium is treated in the form of springs. Later on, the uncertainties involved in the analysis are treated as fuzzy variables and are propagated in the EFGM using vertex method of function approximation. The EFGM employs moving least square approximants to approximate the function. Results of the proposed method are compared with analytical solutions. Numerical Example 1 and Example 2 are used to study the accuracy and convergence of the EFGM in which subgrade modulus and applied load are treated as fuzzy variables.

Element Free Galerkin Method

The element free Galerkin method is one of the meshfree methods developed by Belytschko et al. (1994) based on the diffuse elements method (DEM) originated by Nayroles et al. (1992). In the original EFGM (Belytschko et al. 1994; Lu et al. 1994; Lu et al. 1995), the meshless shape functions do not represent interpolation functions. Hence, the essential boundary conditions cannot be imposed exactly due to loss of delta function property. Initially, Belytschko et al. (1994) employed the general Lagrange multipliers approach to impose the boundary conditions. This requires solution of the Lagrange multipliers in addition to the discrete field variables. This leads to a larger size of the system matrix, loss of the bandedness of the system matrix, and an awkward linear equation structure. The matrix, which has to be inverted, possesses zeroes in the diagonal elements and thus may require special solvers that cannot utilize the positive-definiteness of the system matrix. Subsequently, Lu et al. (1994) proposed a modified variational principle in which Lagrange multipliers are replaced by their physical meaning. Although this leads to banded set of equations, (but not necessarily positive-definite matrices), the results are not as accurate when compared with those by the Lagrange multipliers approach. Another approach proposed by Krongauz and Belytschko (1996) is to necklace the EFGM domain with the FEM domain and apply the boundary conditions to the finite element nodes. This coupling technique dramatically simplifies the enforcement of boundary conditions, but compromises the salient features of the EFGM (Liu 2000). Kaljevic and Saigal (1995) introduced a singular weight function into the moving least-squares approximation to reproduce the Kronecker-delta properties. This technique thus allows the enforcement of essential boundary conditions more efficiently. Methods based on penalty functions and alternative definitions of discrete norm have also been reported (Atluri 1998; Sukumar 2001; Shepard 1968). Rao and

Rahman (2000) have used the transformation method for the imposition of essential boundary conditions in the EFGM.

The major features of the EFGM used in the present paper are as follows:

1. Generalized moving least square approximation is employed for the construction of the shape function.
2. Galerkin weak form is employed to develop the discretized system of equations.
3. Cells of the background mesh for integration are required to carry out the integration to calculate system matrices.

It should be noted that the moving least squares approximation is based only on the information of the values (fictitious values) of the variables at some scattered points (Atluri and Zhu 1998). However, information concerning the derivatives of variables at some scattered points may be meaningful in some physical cases, and if they are used in an approximation procedure, it may give a better approximation result than the procedure that does not use the derivative information. From this point of view, the EFGM is presented in this paper which employs the generalized moving least square approximants to approximate the function and the transformation matrix for imposing the essential boundary conditions.

Generalized Moving Least Squares Approximation

Generalized Moving Least Squares (GMLS) (Atluri et. al. 1999) approximations are used to construct the EFGM shape functions. Consider a function, u(x) over a domain, $\Omega \subseteq \Re^K$, where K = 1, 2, or 3. Let $\Omega_x \subseteq \Omega$ denote a sub-domain describing the neighbourhood of a point, $\boldsymbol{x} \in \Re^K$ located in Ω. According to the generalized moving least squares the approximation, $u^h(\boldsymbol{x})$ of u(x) is

$$u^h(\boldsymbol{x}) = \sum_{i=1}^{m} p_i(\boldsymbol{x}) a_i(\boldsymbol{x}) + \frac{\partial p_i(\boldsymbol{x})}{\partial x} a_i(\boldsymbol{x}) = \boldsymbol{p}^T(\boldsymbol{x})\boldsymbol{a}(\boldsymbol{x}) + \boldsymbol{p}_x^T(\boldsymbol{x})\boldsymbol{a}(\boldsymbol{x}) \tag{1}$$

where

$\boldsymbol{p}^T(\boldsymbol{x}) = \{p_1(\boldsymbol{x}), p_2(\boldsymbol{x}), \cdots, p_m(\boldsymbol{x})\}$ and $\boldsymbol{p}_x^T(\boldsymbol{x}) = \left\{\frac{\partial p_1(\boldsymbol{x})}{\partial x}, \frac{\partial p_2(\boldsymbol{x})}{\partial x}, \cdots, \frac{\partial p_m(\boldsymbol{x})}{\partial x}\right\}$ are respectively the m^{th} order vectors of complete basis functions and derivative of basis functions with respect to x, and $\boldsymbol{a}(\boldsymbol{x}) = \{a_1(\boldsymbol{x}), a_2(\boldsymbol{x}), \cdots, a_m(\boldsymbol{x})\}$ is a vector of unknown parameters that depend on x. The basis functions should satisfy the following properties: (1) p1(x) = 1, (2) $p_i(\boldsymbol{x}) \in C^s(\Omega)$, $i = 1, 2, \cdots, m$ where $C^s(\Omega)$ is a set of functions that have continuous derivatives up to order s on Ω, and (3) $p_i(\boldsymbol{x}), i = 1, 2, \cdots, m$ constitute a linearly independent set. For example in one dimension, the $(m-1)^{\text{th}}$ order polynomial basis and its derivative with respect to x has the following form

$$\boldsymbol{p}^T(x)=\left\{1,\, x,\, x^2,\cdots,\, x^{m-1}\right\} \tag{2}$$

$$\boldsymbol{p}_x^T(\boldsymbol{x})=\left\{0,1,2x,\cdots,(m-1)x^{m-2}\right\} \tag{3}$$

and the vector of undetermined coefficients has the following form in one dimension.

$$\boldsymbol{a}(x)=\left\{a_1(x),a_2(x),\cdots,a_{m-1}(x)\right\} \tag{4}$$

In Equation (1), the coefficient vector, $\boldsymbol{a}(\boldsymbol{x})$ in one dimension is determined by minimizing a weighted discrete $\mathcal{L}_2$ norm, defined as

$$J(x) \;=\; \sum_{I=1}^{n} w_I(x)\left[\boldsymbol{p}^T(x_I)\boldsymbol{a}(x)-\hat{u}_I\right]^2+w_I(x)\left[\boldsymbol{p}_x^T(x_I)\boldsymbol{a}(x)-\hat{\theta}_I\right]^2 \tag{5}$$

where x_I denotes the coordinates of node *I*, $\hat{u}_I$ and $\hat{\theta}_I$ denote $u(x_I)$, and $\dfrac{\partial u(x_I)}{\partial x}$, respectively, $w_I(\boldsymbol{x})$ denotes the weight function associated with node I such that $w_I(\boldsymbol{x})\geq 0$ for all $\boldsymbol{x}$ in the support Ω_x of $w_I(x)$ and zero otherwise, *n* is the number of nodes in Ω_x for which $w_I(x)>0$. Note that $\hat{u}_I$ and $\hat{\theta}_I$ represent the nodal parameters (not the nodal values of $u^h(x)$ and $\dfrac{\partial u^h(x)}{\partial x}$ respectively, in one dimension) for node *I*. Using the matrix notation, Equation (5) can be rewritten as

$$\begin{aligned} J(\boldsymbol{x}) &= \left[\boldsymbol{P}\boldsymbol{a}(\boldsymbol{x})-\hat{\boldsymbol{u}}\right]^T\boldsymbol{W}\left[\boldsymbol{P}\boldsymbol{a}(\boldsymbol{x})-\hat{\boldsymbol{u}}\right]+\left[\boldsymbol{P}_x\boldsymbol{a}(\boldsymbol{x})-\hat{\boldsymbol{\theta}}\right]^T\boldsymbol{W}\left[\boldsymbol{P}_x\boldsymbol{a}(\boldsymbol{x})-\hat{\boldsymbol{\theta}}\right] \\ &= \left[\begin{Bmatrix}\boldsymbol{P}\\ \boldsymbol{P}_x\end{Bmatrix}\boldsymbol{a}(\boldsymbol{x})-\begin{Bmatrix}\hat{\boldsymbol{u}}\\ \hat{\boldsymbol{\theta}}\end{Bmatrix}\right]^T\begin{bmatrix}\boldsymbol{W} & 0\\ 0 & \boldsymbol{W}\end{bmatrix}\left[\begin{Bmatrix}\boldsymbol{P}\\ \boldsymbol{P}_x\end{Bmatrix}\boldsymbol{a}(\boldsymbol{x})-\begin{Bmatrix}\hat{\boldsymbol{u}}\\ \hat{\boldsymbol{\theta}}\end{Bmatrix}\right] \end{aligned} \tag{6}$$

where $\hat{\boldsymbol{u}}^T=\left[\hat{u}_1,\hat{u}_2,\cdots,\hat{u}_n\right]^T$, $\hat{\boldsymbol{\theta}}^T=\left[\hat{\theta}_1,\hat{\theta}_2,\cdots,\hat{\theta}_n\right]^T$,

$\boldsymbol{W}=\mathrm{diag}\left[w_1(\boldsymbol{x}),w_2(\boldsymbol{x}),\cdots,w_N(\boldsymbol{x})\right]$,

$$\boldsymbol{P}=\begin{bmatrix}\boldsymbol{p}^T(x_1)\\ \boldsymbol{p}^T(x_2)\\ \vdots\\ \boldsymbol{p}^T(x_n)\end{bmatrix}\in\mathcal{L}\left(\Re^n\times\Re^m\right) \tag{7}$$

and

$$\boldsymbol{P}_x = \begin{bmatrix} \boldsymbol{p}_x^T(x_1) \\ \boldsymbol{p}_x^T(x_2) \\ \vdots \\ \boldsymbol{p}_x^T(x_n) \end{bmatrix} \in \mathcal{L}\left(\Re^n \times \Re^m\right) \tag{8}$$

The stationarity of $J(x)$ with respect to $\boldsymbol{a}(x)$ yields

$$\boldsymbol{A}(x)\boldsymbol{a}(x) = \boldsymbol{C}(x)\boldsymbol{d} \tag{9}$$

where

$$\boldsymbol{A}(x) \equiv \sum_{I=1}^{n} w_I(x)\boldsymbol{p}(x_I)\boldsymbol{p}^T(x_I) + w_I(x)\boldsymbol{p}_x(x_I)\boldsymbol{p}_x^T(x_I) = \boldsymbol{P}^T\boldsymbol{W}\boldsymbol{P} + \boldsymbol{P}_x^T\boldsymbol{W}\boldsymbol{P}_x \tag{10}$$

$$\begin{aligned} \boldsymbol{C}(x) &\equiv \left[w_1(x)\boldsymbol{p}(x_1), \cdots, w_n(x)\boldsymbol{p}(x_n), w_1(x)\boldsymbol{p}_x(x_1), \cdots, w_n(x)\boldsymbol{p}_x(x_n)\right] \\ &= \left[\boldsymbol{P}^T\boldsymbol{W}, \boldsymbol{P}_x^T\boldsymbol{W}\right] \end{aligned} \tag{11}$$

and

$$\boldsymbol{d} \equiv \left\{\hat{\boldsymbol{u}}, \quad \hat{\boldsymbol{\theta}}\right\}^T = \left\{\hat{u}_1, \hat{u}_2, \cdots, \hat{u}_n, \quad \hat{\theta}_1, \hat{\theta}_2, \cdots, \hat{\theta}_n\right\}^T \tag{12}$$

Solving $\boldsymbol{a}(x)$ from Equation (9) and then substituting it in Equation (1) gives

$$u^h(x) = \sum_{I=1}^{n} \phi_{uI}(x)\hat{u}_I + \phi_{\theta I}(x)\hat{\theta}_I = \boldsymbol{\Phi}_u^T(x)\hat{\boldsymbol{u}} + \boldsymbol{\Phi}_\theta^T(x)\hat{\boldsymbol{\theta}} \tag{13}$$

where

$$\begin{aligned} \boldsymbol{\Phi}_u^T(x) &= \boldsymbol{p}(x)\boldsymbol{A}^{-1}(x)\boldsymbol{P}^T\boldsymbol{W} \\ \boldsymbol{\Phi}_\theta^T(x) &= \boldsymbol{p}(x)\boldsymbol{A}^{-1}(x)\boldsymbol{P}_x^T\boldsymbol{W} \end{aligned} \tag{14}$$

or I^{th} component of $\boldsymbol{\Phi}_u^T(x)$ and $\boldsymbol{\Phi}_\theta^T(x)$ are respectively,

$$\begin{aligned} \phi_{uI}(x) &= \sum_{j=1}^{m} p_j(x)\left[\boldsymbol{A}^{-1}(x)\boldsymbol{P}^T\boldsymbol{W}\right]_{jI} \\ \phi_{\theta I}(x) &= \sum_{j=1}^{m} p_j(x)\left[\boldsymbol{A}^{-1}(x)\boldsymbol{P}_x^T\boldsymbol{W}\right]_{jI} \end{aligned} \tag{15}$$

representing the shape function of the GMLS approximation of $u^h(x)$ and $\dfrac{\partial u^h(x)}{\partial x}$ respectively, corresponding to node *I*. The partial derivatives of $\phi_{uI}(x)$ and $\phi_{\theta I}(x)$ can be obtained as follows

$$\frac{\partial \phi_{uI}(x)}{\partial x} = \sum_{j=1}^{m} \frac{\partial p_j(x)}{\partial x} \left[\boldsymbol{A}^{-1}(x) \boldsymbol{P}^T \boldsymbol{W} \right]_{jI} + \sum_{j=1}^{m} p_j(x) \frac{\partial \left[\boldsymbol{A}^{-1}(x) \boldsymbol{P}^T \boldsymbol{W} \right]_{jI}}{\partial x}$$
$$\frac{\partial \phi_{\theta I}(x)}{\partial x} = \sum_{j=1}^{m} \frac{\partial p_j(x)}{\partial x} \left[\boldsymbol{A}^{-1}(x) \boldsymbol{P}_x^T \boldsymbol{W} \right]_{jI} + \sum_{j=1}^{m} p_j(x) \frac{\partial \left[\boldsymbol{A}^{-1}(x) \boldsymbol{P}_x^T \boldsymbol{W} \right]_{jI}}{\partial x} \tag{16}$$

where

$$\boldsymbol{A}_{,i}^{-1} = -\boldsymbol{A}^{-1} \boldsymbol{A}_{,i} \boldsymbol{A}^{-1} \tag{17}$$

in which $(\,)_{,i} = \frac{\partial (\,)}{\partial x_i}$.

Weight Function

An important ingredient of the EFGM or other meshless methods is the weight function, *w*(*x*). The choice of the weight function can affect the MLS approximation of $u^h(\boldsymbol{x})$ (Rao and Rahaman 2000). In this work, weight function based on the student's *t*-distribution is adopted (Rao and Rahaman 2000). It is given by

$$w_I(\boldsymbol{x}) = \begin{cases} \dfrac{\left(1+\beta^2 \dfrac{z_I^2}{z_{mI}^2}\right)^{-\left(\frac{1+\beta}{2}\right)} - \left(1+\beta^2\right)^{-\left(\frac{1+\beta}{2}\right)}}{1-\left(1+\beta^2\right)^{-\left(\frac{1+\beta}{2}\right)}}, & z_I \le z_{mI} \\ 0, & z_I > z_{mI} \end{cases} \tag{18}$$

where β is the parameter controlling the shape of the weight function, $z_I = \| \boldsymbol{x} - \boldsymbol{x}_I \|$ is the distance from a sampling point, $\boldsymbol{x}$ to a node $\boldsymbol{x}_I$, z_{mI} is the domain of influence of node I such that

$$z_{mI} = z_{\max} z_{cI} \tag{19}$$

in which z_{cI} is a the characteristic nodal spacing distance which is chosen such that the node I has enough number of neighbours sufficient to guarantee a non-singular matrix $\boldsymbol{A}(\boldsymbol{x})$ in Equation (9) (which is used to determine the GMLS approximation), and $z_{\max}$ is a scaling parameter.

Variational Formulation and Discretization

A governing equation for beam on an elastic foundation is given by the following 4th order differential equation,

$$EIu_{,xxxx} + k_s(x)u = q(x) \text{ in } \Omega = (0, L) \tag{20}$$

where u is transverse displacement, EI is flexural rigidity, k_s is the foundation stiffness, and $q(x)$ is distributed load over the beam. The boundary conditions are given at the global boundary, Γ, as

$$\begin{aligned} &u(0)=0, \quad \theta(0)=0 \\ &M(L)=EIu_{,xx}(L)=0 \\ &V(L)=-EIu_{,xxx}(L)=0 \end{aligned} \tag{21}$$

To obtain the discrete equations it is first necessary to use a weak form of the equilibrium equation and boundary conditions. The variational or weak form of Equations (20) and (21) is

$$\int_0^L EIu_{,xx}v_{,xx}dx = \int_0^L qvdx - \int_0^L k_s(x)uvdx + EIu_{,xxx}v\Big|_{x=0} - EIu_{,xx}v_{,x}\Big|_{x=0} \tag{22}$$

where the trial function $u(x)$ and the test function $v(x)$ are such that $u \in S \quad \forall \quad v \in V$ where $S \equiv \{u \mid u \in H^2, u = g \text{ on } x=0\}$, and $V \equiv \{v \mid v \in H^2, v = 0 \text{ on } x=0\}$ with $g = 0$.

From Equation 13, the GMLS approximation of $u(x_J)$, $\frac{\partial u(x_J)}{\partial x}$, and $\frac{\partial^2 u(x_J)}{\partial x^2}$ are respectively,

$$u^h(x_J) = \sum_{I=1}^{n} \phi_{uI}(x_J)\hat{u}_I + \phi_{\theta I}(x_J)\hat{\theta}_I = \boldsymbol{\Phi}_u^T(x_J)\hat{\boldsymbol{u}} + \boldsymbol{\Phi}_\theta^T(x_J)\hat{\boldsymbol{\theta}} \tag{23}$$

$$\begin{aligned} \frac{\partial u^h(x_J)}{\partial x} \equiv \theta^h(x_J) &= \sum_{I=1}^{n} \frac{\partial \phi_{uI}(x)}{\partial x}(x_J)\hat{u}_I + \frac{\partial \phi_{\theta I}(x)}{\partial x}(x_J)\hat{\theta}_I \\ &= \frac{\partial \boldsymbol{\Phi}_u^T(x_J)}{\partial x}\hat{\boldsymbol{u}} + \frac{\partial \boldsymbol{\Phi}_\theta^T(x_J)}{\partial x}\hat{\boldsymbol{\theta}} \end{aligned} \tag{24}$$

and

$$\frac{\partial^2 u^h(x_J)}{\partial x^2} = \sum_{I=1}^{n} \frac{\partial^2 \phi_{uI}(x)}{\partial x^2}(x_J)\hat{u}_I + \frac{\partial^2 \phi_{\theta I}(x)}{\partial x^2}(x_J)\hat{\theta}_I = \frac{\partial^2 \boldsymbol{\Phi}_u^T(x_J)}{\partial x^2}\hat{\boldsymbol{u}} + \frac{\partial^2 \boldsymbol{\Phi}_\theta^T(x_J)}{\partial x^2}\hat{\boldsymbol{\theta}} \tag{25}$$

Equations (23) and (24) can be rewritten in a matrix form as

$$\begin{Bmatrix} u^h(x_J) \\ \theta^h(x_J) \end{Bmatrix} = \sum_{I=1}^{n} \begin{bmatrix} \phi_{uI}(x_J) & \phi_{\theta I}(x_J) \\ \dfrac{\partial \phi_{uI}(x)}{\partial x} & \dfrac{\partial \phi_{\theta I}(x)}{\partial x} \end{bmatrix} \begin{Bmatrix} \hat{u}_I \\ \hat{\theta}_I \end{Bmatrix} \tag{26}$$

Equations (26) can be written for all nodes as

$$\hat{\boldsymbol{d}} = \mathbf{L}\,\bar{\boldsymbol{d}} \tag{27}$$

where

$$\hat{\boldsymbol{d}} = \begin{Bmatrix} u^h(x_1) \\ \theta^h(x_1) \\ u^h(x_2) \\ \theta^h(x_2) \\ \vdots \\ u^h(x_N) \\ \theta^h(x_N) \end{Bmatrix} \in \Re^{2N} \tag{28}$$

is the nodal displacement vector,

$$\overline{\boldsymbol{d}} = \begin{Bmatrix} \hat{u}^h(x_1) \\ \hat{\theta}^h(x_1) \\ \hat{u}^h(x_2) \\ \hat{\theta}^h(x_2) \\ \vdots \\ \hat{u}^h(x_N) \\ \hat{\theta}^h(x_N) \end{Bmatrix} \in \Re^{2N} \tag{29}$$

is the nodal parameters vector, and

$$\mathbf{L} = \begin{bmatrix} \phi_{u1}(x_1) & \phi_{\theta 1}(x_1) & \phi_{u2}(x_1) & \phi_{\theta 2}(x_1) & \cdots & \phi_{uN}(x_1) & \phi_{\theta N}(x_1) \\ \frac{\partial \phi_{u1}(x_1)}{\partial x} & \frac{\partial \phi_{\theta 1}(x_1)}{\partial x} & \frac{\partial \phi_{u2}(x_1)}{\partial x} & \frac{\partial \phi_{\theta 2}(x_1)}{\partial x} & \cdots & \frac{\partial \phi_{uN}(x_1)}{\partial x} & \frac{\partial \phi_{\theta N}(x_1)}{\partial x} \\ \phi_{u1}(x_2) & \phi_{\theta 1}(x_2) & \phi_{u2}(x_2) & \phi_{\theta 2}(x_2) & \cdots & \phi_{uN}(x_2) & \phi_{\theta N}(x_2) \\ \frac{\partial \phi_{u1}(x_2)}{\partial x} & \frac{\partial \phi_{\theta 1}(x_2)}{\partial x} & \frac{\partial \phi_{u2}(x_2)}{\partial x} & \frac{\partial \phi_{\theta 2}(x_2)}{\partial x} & \cdots & \frac{\partial \phi_{uN}(x_2)}{\partial x} & \frac{\partial \phi_{\theta N}(x_2)}{\partial x} \\ \vdots & \vdots & \vdots & \vdots & \cdots & \vdots & \vdots \\ \phi_{u1}(x_N) & \phi_{\theta 1}(x_N) & \phi_{u2}(x_N) & \phi_{\theta 2}(x_N) & \cdots & \phi_{uN}(x_N) & \phi_{\theta N}(x_N) \\ \frac{\partial \phi_{u1}(x_N)}{\partial x} & \frac{\partial \phi_{\theta 1}(x_N)}{\partial x} & \frac{\partial \phi_{u2}(x_N)}{\partial x} & \frac{\partial \phi_{\theta 2}(x_N)}{\partial x} & \cdots & \frac{\partial \phi_{uN}(x_N)}{\partial x} & \frac{\partial \phi_{\theta N}(x_N)}{\partial x} \end{bmatrix} \equiv \begin{bmatrix} \boldsymbol{\Psi}^T(x_1) \\ \frac{\partial \boldsymbol{\Psi}^T(x_1)}{\partial x} \\ \boldsymbol{\Psi}^T(x_2) \\ \frac{\partial \boldsymbol{\Psi}^T(x_2)}{\partial x} \\ \vdots \\ \boldsymbol{\Psi}^T(x_N) \\ \frac{\partial \boldsymbol{\Psi}^T(x_N)}{\partial x} \end{bmatrix} \in \mathcal{L}\left(\Re^{2N} \times \Re^{2N}\right) \tag{30}$$

is the transformation matrix. Therefore the GMLS approximation of $u(x)$, $\frac{\partial u(x)}{\partial x}$, and $\frac{\partial^2 u(x)}{\partial x^2}$, can be rewritten respectively, as follows

$$u^h(x)=\sum_I \boldsymbol{\Psi}^T(x)\bar{\boldsymbol{d}}_I=\left\{\phi_{u1}(x)\quad \phi_{\theta 1}(x)\quad \phi_{u2}(x)\quad \phi_{\theta 2}(x)\quad \cdots\quad \phi_{uN}(x)\quad \phi_{\theta N}(x)\right\}\bar{\boldsymbol{d}}=\boldsymbol{\Psi}^T(x)\mathbf{L}^{-1}\hat{\boldsymbol{d}} \tag{31}$$

$$\frac{\partial u^h(x)}{\partial x}=\sum_I \frac{\partial \boldsymbol{\Psi}(x)}{\partial x}\bar{\boldsymbol{d}}_I=\left\{\frac{\partial\phi_{u1}(x)}{\partial x}\quad \frac{\partial\phi_{\theta 1}(x)}{\partial x}\quad \frac{\partial\phi_{u2}(x)}{\partial x}\quad \frac{\partial\phi_{\theta 2}(x)}{\partial x}\quad \cdots\quad \frac{\partial\phi_{uN}(x)}{\partial x}\quad \frac{\partial\phi_{\theta N}(x)}{\partial x}\right\}\bar{\boldsymbol{d}}=\frac{\partial \boldsymbol{\Psi}(x)}{\partial x}\mathbf{L}^{-1}\hat{\boldsymbol{d}} \tag{32}$$

$$\frac{\partial^2 u^h(x)}{\partial x^2}=\sum_I \frac{\partial^2 \boldsymbol{\Psi}(x)^T}{\partial x^2}\bar{\boldsymbol{d}}_I=\left\{\frac{\partial^2\phi_{u1}(x)}{\partial x^2}\quad \frac{\partial^2\phi_{\theta 1}(x)}{\partial x^2}\quad \frac{\partial^2\phi_{u2}(x)}{\partial x^2}\quad \frac{\partial^2\phi_{\theta 2}(x)}{\partial x^2}\quad \cdots\quad \frac{\partial^2\phi_{uN}(x)}{\partial x^2}\quad \frac{\partial^2\phi_{\theta N}(x)}{\partial x^2}\right\}\bar{\boldsymbol{d}}=\frac{\partial^2 \boldsymbol{\Psi}(x)^T}{\partial x^2}\mathbf{L}^{-1}\hat{\boldsymbol{d}} \tag{33}$$

Similarly,

$$v^h(x)=\boldsymbol{\Psi}^T(x)\mathbf{L}^{-1}\hat{\boldsymbol{v}} \tag{34}$$

$$\frac{\partial v^h(x)}{\partial x}=\frac{\partial \boldsymbol{\Psi}^T(x)}{\partial x}\mathbf{L}^{-1}\hat{\boldsymbol{v}} \tag{35}$$

$$\frac{\partial^2 v^h(x)}{\partial x^2}=\frac{\partial^2 \boldsymbol{\Psi}^T(x)}{\partial x^2}\mathbf{L}^{-1}\hat{\boldsymbol{v}} \tag{36}$$

where $\hat{\boldsymbol{v}}$ is the discretized nodal test function vector similar to the nodal displacement vector $\hat{\boldsymbol{d}}$.

Using Equations (31) – (36) into the discretization of Equation (22) gives

$$\hat{\boldsymbol{K}}\hat{\boldsymbol{d}}=\hat{\boldsymbol{f}} \tag{37}$$

where

$$\hat{\boldsymbol{K}}=\boldsymbol{\Lambda}^{-T}\begin{bmatrix}\boldsymbol{k}_{11} & \boldsymbol{k}_{12} & \cdots & \boldsymbol{k}_{1N}\\ \boldsymbol{k}_{21} & \boldsymbol{k}_{22} & \cdots & \boldsymbol{k}_{2N}\\ \vdots & \vdots & \vdots & \vdots\\ \boldsymbol{k}_{N1} & \boldsymbol{k}_{N2} & \cdots & \boldsymbol{k}_{NN}\end{bmatrix}\boldsymbol{\Lambda}^{-1}\in\mathcal{L}\left(\Re^{2N}\times\Re^{2N}\right) \tag{38}$$

is the stiffness matrix with

$$\boldsymbol{k}_{IJ}=\int_\Omega \boldsymbol{B}_I^T EI\boldsymbol{B}_J\,d\Omega\ +\int_\Omega \boldsymbol{\Psi}_I^T k_s\boldsymbol{\Psi}_J\,d\Omega\ \in\mathcal{L}\left(\Re^2\times\Re^2\right) \tag{39}$$

representing the contributions of J^{th} node at node I with

$$\boldsymbol{B}_I^T=\begin{Bmatrix}\dfrac{\partial^2\phi_{uI}(x)}{\partial x^2}\\ \dfrac{\partial^2\phi_{\theta I}(x)}{\partial x^2}\end{Bmatrix}\ \text{and}\ \boldsymbol{\Psi}_I^T=\begin{Bmatrix}\phi_{uI}(x)\\ \phi_{\theta I}(x)\end{Bmatrix},\ \hat{\boldsymbol{f}}=\boldsymbol{\Lambda}^{-T}\boldsymbol{f}\in\Re^{2N} \tag{40}$$

is the force vector with

$$\boldsymbol{f}_I = \int_0^L \boldsymbol{\Psi}_I^T q(x)\,dx \; + \left[\boldsymbol{\Psi}_I^T EIu_{,xxx}\right]_{x=0} - \left[\frac{\partial \boldsymbol{\Psi}_I^T}{\partial x} EIu_{,xx}\right]_{x=0} \in \mathcal{L}\left(\Re^2 \times \Re^2\right) \tag{41}$$

with $$\frac{\partial \boldsymbol{\Psi}_I^T}{\partial x} = \begin{Bmatrix} \dfrac{\partial \phi_{uI}(x)}{\partial x} \\ \dfrac{\partial \phi_{\theta I}(x)}{\partial x} \end{Bmatrix}$$

Noting that $\hat{\boldsymbol{d}}$ in Equation (37) is the nodal displacement vector, the discretized linear equation system in Equation (37) can be solved for the unknown nodal displacements u_I and rotations θ_I and the internal forces after applying appropriate essential boundary conditions by adopting the procedures similar to that in finite element analysis. The proposed method of applying essential boundary conditions using the transformation matrix avoids some of the drawbacks of Lagrange multiplier technique and modified variational principle approach (Belytschko et al. 1996) such as larger size of the system matrix, loss of the bandedness of the system matrix in case of Lagrange multiplier technique and non-positive definite matrices in case of modified variational principle approach.

Interval Analysis Using Vertex Method

Traditionally, probability theory has been the primary tool for representing uncertainty in geotechnical engineering. Because of this, all uncertainty associated with geotechnical engineering problems was assumed to follow the characteristics of random uncertainty. However, not all uncertainty is random and hence nonrandom uncertainty is not suited to modelling by probability theory. Fuzzy set theory provides a means for representing nonrandom uncertainties associated with vagueness, with imprecision and/or with a lack of information regarding a particular element of the problem under investigation (Zadeh 1965).

The extension principle, introduced by Zadeh (1978), is one of the most important tools of fuzzy set theory. This principle allows the generalization of crisp mathematical concepts to the fuzzy set framework and extends point-to-point mappings to mappings for fuzzy sets. It provides a means for any function f that maps an n-tuple (x_1, x_2,..., x_n) in the crisp set X to a point in the crisp set Y to be generalized to mapping n fuzzy subsets in X to a fuzzy set in Y. Hence, any mathematical relationships between nonfuzzy elements can be extended to deal with fuzzy entities. Vertex method greatly simplifies the manipulations of the extension principle for continuous-valued fuzzy variables such as fuzzy numbers defined on the real line. The method is based on the combination of the λ- cut concept and standard interval analysis. Vertex method can prevent the abnormality in the output membership function due to the application of discretization technique on the fuzzy variables domain, and it can prevent the widening of the resulting function value set due to multiple occurrences of variables in the functional expression by conventional interval analysis methods (Dong and Shah 1987). The algorithm is very easy to implement and works as follows. The algorithm works. Any continuous membership function can be represented by a continuous sweep of λ- cut from $\lambda = 0^+$ to $\lambda = 1$. Figure 1

shows a typical membership function with an interval associated with a specific value of λ.

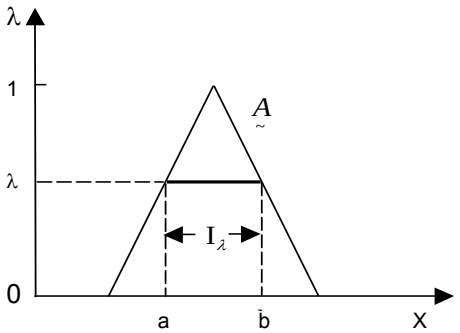

Fig. 1 Interval Corresponding to a λ- Cut Level on Fuzzy Set $\underset{\sim}{A}$

Suppose there is a single-input mapping given by $y = f(x)$ that is to be extended for the fuzzy sets, or $\underset{\sim}{B} = f\left(\underset{\sim}{A}\right)$,and needs to decompose $\underset{\sim}{A}$ in to a series of λ- cut intervals, say I_λ. When the function $f(x)$ is a continuous and monotonic on $I_\lambda = [a, b]$, the interval represented $\underset{\sim}{B}$ at a particular value of λ, say B_λ , can be obtained by

$$B_\lambda = f(I_\lambda) = \left[\min(f(a), f(b)),\ \max(f(a), f(b))\right] \tag{42}$$

Equation (42) has reduced the interval analysis problem for a functional mapping to a simple procedure dealing only with the endpoints of the interval. When the mapping is given by *n* inputs, i.e., $y = f(x_1, x_2, ..., x_n)$, then the input space can be represented by an *n*-dimensional Cartesian region. Each of the input variables can be described by an interval, say $I_{i\lambda}$, at a specific λ- cut, where

$$I_{i\lambda} = [a_i, b_i] \qquad i = 1, 2, ..., n \tag{43}$$

The endpoint pairs of each interval given in Equation (42) intersect in the 2D space and form the vertex of the Cartesian space. The coordinates of these vertices are the values used in the vertex method when determining the output interval for each λ- cut. The number of vertices, *N,* is a quantity equal to $N = 2^n$, where *n* is the number of fuzzy input variables. When the mapping $y = f(x_1, x_2, ..., x_n)$ is continuous in the *n*-dimensional Cartesian region and when also there is no extreme point in this region, the value of the interval function for a particular λ- cut can be obtained by

$$B_\lambda = f(I_{1\lambda}, I_{2\lambda}, ..., I_{n\lambda}) = \left[\min_j(f(c_j)), \max_j(f(c_j))\right] \quad j = 1, 2, ..., n \tag{44}$$

The vertex method is accurate only when the conditions of continuity and no extreme point are satisfied. When extreme points of the function $y = f(x_1, x_2, ..., x_n)$ exist in the *n*-dimensional Cartesian region of the input parameters, the vertex method will miss certain parts of the interval that should be included in the output interval value, B_λ. Extreme points can be missed, for example, in certain mappings treated as additional vertices, E_k, in the Cartesian space and Equation (44) becomes, because the continuity property still holds,

$$B_\lambda = \left[\min_{j,k}(f(c_j), f(E_k)), \max_{j,k}(f(c_j), f(E_k)) \right] \tag{45}$$

where $j = 1, 2, ..., N$ and $k = 1, 2, ..., m$ for *m* extreme points in the region.

Numerical Example 1: Validation

This example is used to validate the computer program developed for fuzzy meshless analysis of beams on elastic foundation. In this case, a deterministic analysis is carried out with four different values of 2L such that μL = 1, 2, 3, and 4 where $\mu = \sqrt[4]{\frac{k_s}{4EI}}$. A third order polynomial basis function and β = 4 are used in all the numerical examples. Due to symmetry, only half of the beam is analyzed. The domain of the beam is divided into cells with their nodes coinciding with the meshless nodes solely for numerical integration. For numerical integration, a 8-point Gauss quadrature rule is used for all the cells of the background mesh. Validation example considers a finite beam with central point load P = 1000 kN as depicted in Figure 2. Parameters considered in analysis are: length 2L of the beam, flexural rigidity EI of the beam = 22360.68 kN–m^2 and foundation stiffness k_s = 36000 kN/m^3.

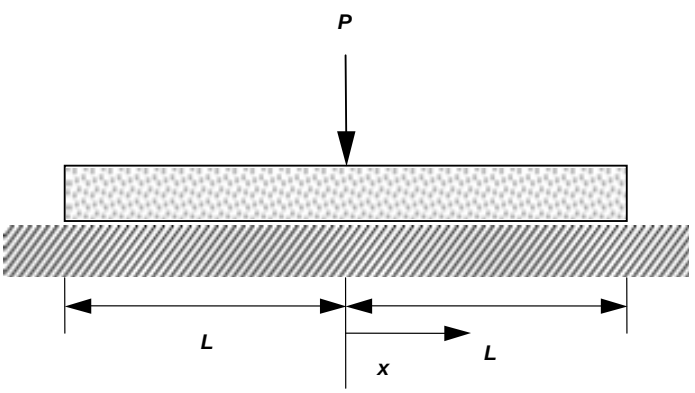

Fig. 2 Beam on Elastic Foundation with Central Point Load

The proposed EFGM is used to obtain the normalized displacement and the normalized bending moment along the length of the beam (2L). The numerical results obtained by the proposed method (Figures 3 and 4) are compared with the analytical solutions available in the literature (Hetenyi 1958).

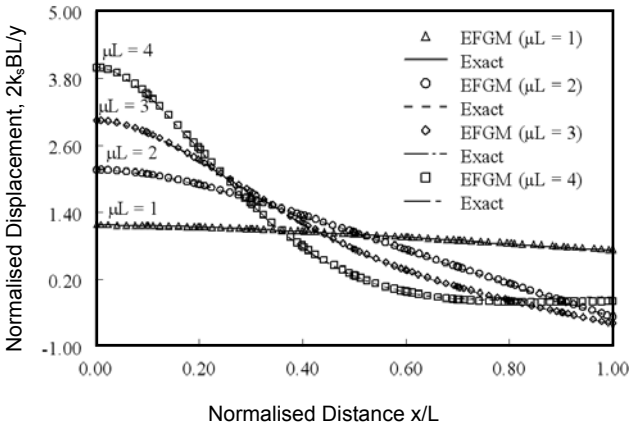

Fig. 3 Normalized Displacement along the Length of Beam with Central Point Load

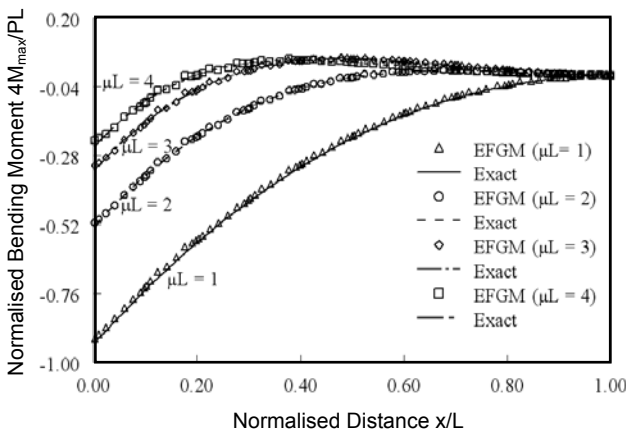

Fig. 4 Normalized Bending Moment along the Length of Beam with Central Point Load Nu

Numerical Example 2:

Finite beam with two point loads at a distance from the centre

This numerical example involves a beam with two point loads placed at distance of 4 m on either side of the centre as depicted in Figure 5. Due to symmetry of the geometry and loading, only half of the beam is analyzed. In the analysis, the subgrade modulus and applied point load are considered as fuzzy

variables and are propagated in the analysis using vertex method. In this example, length of the beam is L (20 m), flexural rigidity EI of the beam is 22360.68 kN–m^2 and the fuzzy variables – subgrade modulus k_s is varying from 24000 to 48000 kN/m^3 and applied load is varying from 400 to 1600 kN. A concept of λ-cut along with vertex method are used to evaluate the uncertainty in the output variables.

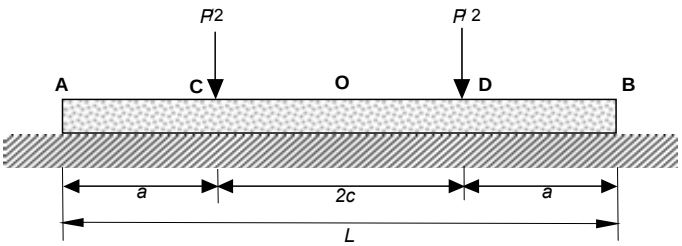

Fig. 5 Beam Subjected to Two Point Loads at a Distance from the Centre

The proposed EFGM is used to obtain the displacement, slope and moment along the length of the beam with four different discretizations consisting of 6, 11, 21 and 41 uniformly spaced meshless nodes over the half length of the beam (L/2). Analytical expressions for the evaluation of displacement, slope and moment under the load (i.e. points C and D) are given as below (Hetenyi 1958):

Deflection under the load:

$$\begin{aligned} y_C = y_D = \frac{p\lambda}{k}\frac{1}{\sinh\lambda l + \sin\lambda l}\Big[& 2\cosh^2\lambda a\left(\cos 2\lambda c + \cosh\lambda l\right) \\ & + 2\cos^2\lambda a\left(\cosh 2\lambda c + \cos\lambda l\right) \\ & + \sinh 2\lambda a\left(\sin 2\lambda c - \sinh\lambda l\right) - \sin 2\lambda a\left(\sinh 2\lambda c - \sin\lambda l\right)\Big] \end{aligned} \tag{46}$$

Slope under the load:

$$\theta_C = -\theta_D = \frac{2p\lambda^2}{k}\frac{\cosh^2\lambda a\sin 2\lambda c - \cos^2\lambda a\sinh 2\lambda c}{\sinh\lambda l + \sin\lambda l} \tag{47}$$

Bending moment under the load:

$$\begin{aligned} M_C = M_D = \frac{p}{4\lambda}\frac{1}{\sinh\lambda l + \sin\lambda l}\Big[& 2\cosh^2\lambda a\left(\cos 2\lambda c + \cosh\lambda l\right) \\ & - 2\cos^2\lambda a\left(\cosh 2\lambda c + \cos\lambda l\right) \\ & - \sinh 2\lambda a\left(\sin 2\lambda c + \sinh\lambda l\right) \\ & - \sin 2\lambda a\left(\sinh 2\lambda c + \sin\lambda l\right)\Big] \end{aligned} \tag{48}$$

Similar analytical expressions for displacements, slopes and moments at the end and at the center are given by Hetenyi (1958).

When compared with these analytical solutions for the displacement, slope and moment at the load points, at the end and at the center of the beam, the predicted values from the EFGM are matching very well. This ensures the accurate formulation of the EFGM for the beams on elastic foundation.

Figures 6 to 8 show respectively the plots of the displacement, y, the slope, dy/dx and the moment M obtained using the deterministic meshless analysis. It is depicted from the plots that as the number of nodes in the EFGM is increased the solutions converged towards the analytical solutions.

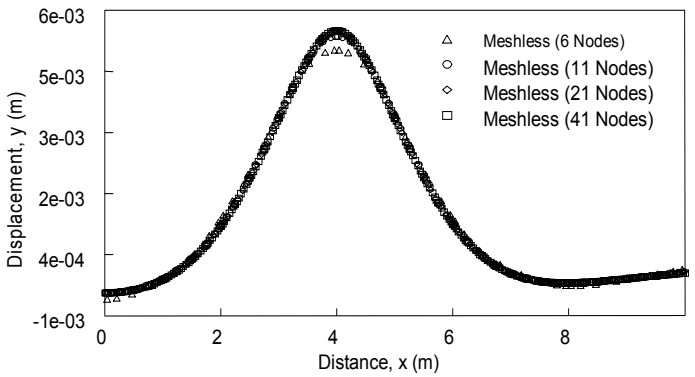

Fig. 6 Displacement along the Length of Beam with Point Loads at a Distance from Center

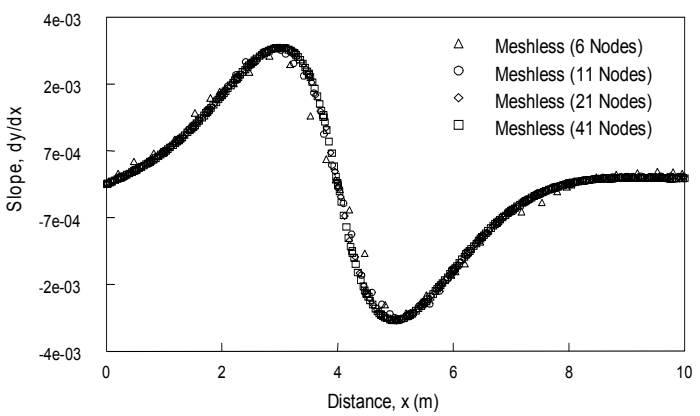

Fig. 7 Slope along the length of Beam with Point loads at Distance from Center

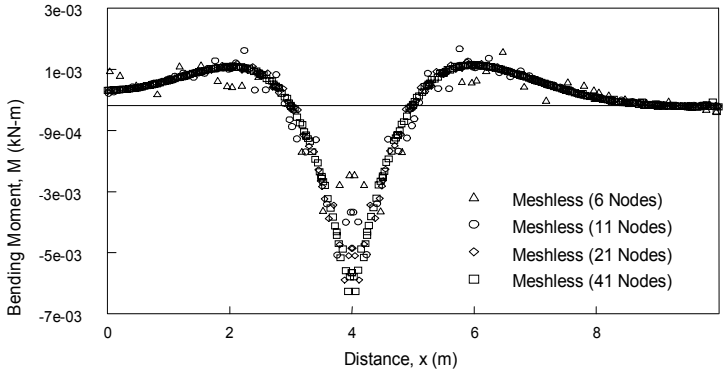

Fig. 8 Bending Moment along the Length of Beam with Point loads at a Distance from Center

The subgrade modulus and applied load are considered as fuzzy variables and their fuzzy sets are constructed using symmetric triangular membership functions. Figures 9 and 10 show the input fuzzy sets for subgrade modulus and applied load respectively. This numerical example is solved using four λ-cut levels namely λ = 0, 1/3, 2/3 and 1. Table 1 gives the results for displacements under the load in the form of fuzzy intervals at each of the λ-cut levels.

Table 1: Displacements at Each λ - Cut Level

λ-cut level	*Subgrade modulus (k_s) (kN/m^3)*	*Applied load (kN)*	*Displacement (mm)*	*Fuzzy interval for displacement at each λ- cut level*
0	24000	400	2.8	12 – 1.786
	24000	1600	12	
	48000	400	1.786	
	48000	1600	7.14	
1/3	28000	600	4	9.36 – 2.86
	28000	1400	2.86	
	44000	600	9.36	
	44000	1400	6.67	
2/3	32000	800	4.84	7.265 – 4.096
	32000	1200	7.265	
	40000	800	4.096	
	40000	1200	6.14	
1	36000	1000	5.542	5.542 – 5.542

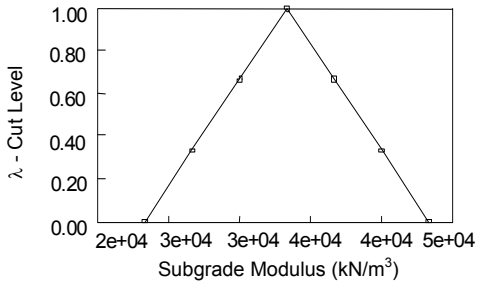

Fig. 9 Input Fuzzy Set for Subgrade Modulus

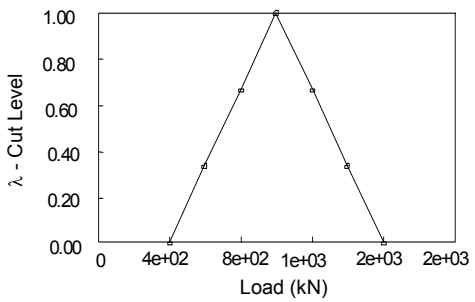

Fig. 10 Input Fuzzy Set for Applied Load

Combinatorial optimization is then performed on the input fuzzy variables to determine the binary combinations of the variables that result in extreme displacements at each λ-cut level using the EFGM. Since, one cannot report the displacement as a fuzzy set, a defuzzification has to be carried out on the displacement output fuzzy set. Defuzzification is the conversion of a fuzzy quantity to a precise quantity. There are several methods for defuzzifying fuzzy output functions in the literature that have been proposed by investigators in recent years (Hellendoorn and Thomas 1993; Dodagoudar and Venkatachalam 2000a; 2000b). For this example, only a displacement output fuzzy set for extreme displacements is shown in Figure 11.

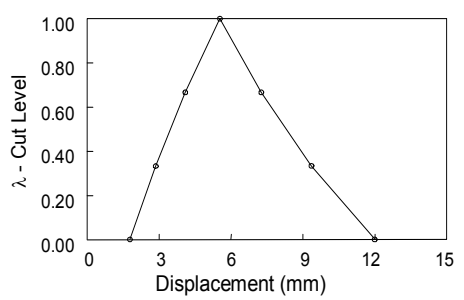

Fig. 11 Output Fuzzy Set for Displacement under the Load

Similarly the output fuzzy sets can be obtained for the slope and bending moment. In this study, centroid method is used to defuzzify all the output fuzzy sets (i.e. displacement, slope and bending moment). The defuzzified value for the displacement output fuzzy set is 5.5942 mm (Table 2).

Table 2: Results for Displacement, Slope and Bending Moment Numerical Example 2

Approaches / *Response Quantities*	*Analytical*	*Meshless Method*	*Fuzzy Meshless Method*
Displacement at end (mm)	0. 025	0.025	0.021
Slope at end (rad)	0.00016	0.00016	0.000158
Bending moment at end (kN-m)	0	0	0
Displacement under the load (mm)	5.542	5.542	5.594
Slope under the load (rad)	0	0	0
Bending moment under the load (kN-m)	157.191	157.191	158.836
Displacement at center (mm)	-0.477	-0.477	-0.489
Slope at center (rad)	0	0	0
Bending moment at center (kN-m)	-12.386	-12.386	-13.507

Comparison of the results for displacements, slopes and bending moments at the end, at the center and under the load for the beam with point loads placed at a distance of 4 m from the center are presented in Table 2. The slope obtained is zero under the load and at the center of the beam for the analytical as well as meshless methods. As expected, the settlement and bending moment are maximum under the load and their corresponding values are 5.5942 mm and 158.836 kN-m.

Discussion

Numerical example 2 is presented to study the applicability of the proposed fuzzy meshless method. An attempt has been made to investigate the performance of the proposed method by carrying out convergence study with the increase of number of meshless nodes. As the number of nodes increased, say 21 meshless nodes, the solution is converged towards the exact solution obtained using analytical expressions given in Hetenyi (1958) for the cases of displacement, slope and bending moment along the beam (Figures 6 to 8). An interval meshless analysis is performed using the vertex method in order to study the influence of fuzzy uncertainty associated with the loading and modulus of subgrade reaction of the soil on the displacement, slope and bending moment. A good comparison is obtained between the results of the EFGM and

analytical solutions for all the above quantities. It is noted from the results that the variation in the input fuzzy variables is small; therefore the uncertainty associated with the resulting quantities evaluated using fuzzy meshless method is small and are almost similar with those evaluated using the deterministic meshless method. In case a significant variation in the input fuzzy uncertainty exists, the resulting quantities will have higher uncertainty in their magnitudes (Sunitha 2007). This information will be used effectively in the design of beams on elastic foundation catering for the input uncertainty.

Summary and Conclusions

The study has demonstrated the applicability of fuzzy meshless method for soil-structure interaction problems such as beams on elastic foundation with uncertain input parameters. The uncertain input parameters are modelled using triangular membership functions and are propagated in the meshless analysis through vertex method of function approximation. In the present study, a systematic methodology has been evolved to combine the EFGM and fuzzy sets approach in the treatment of input fuzzy uncertainty. Displacements are taken as field variables and slope and bending moments are also evaluated as part of the analysis. Unlike the finite element method, the meshless method requires no structured mesh; only a scattered set of nodal points is required in the domain of interest. A numerical example of beam on elastic foundation with point loads placed at equal distance from the center is presented to examine the accuracy and convergence of the meshless method by finding the displacements, slopes and bending moments along the beam. A good agreement is observed between the results of the EFGM and analytical method. This ensures proper formulation of the proposed method for analysing the beams on elastic foundation. Since mesh generation for complex structures is far more time-consuming and costly effort than the solution of a discrete set of equations; the current fuzzy meshless method provides an attractive alternative to finite element method for solving soil-structure interaction problems incorporating cognitive uncertainties. The proposed fuzzy meshless method with some modifications to account for dynamic and wave propagation effects has greater potential for providing solutions to more complex soil-structure interaction problems such as analysis of structures founded on unbounded media including the seismic source effects and path geology in a more comprehensive way. Further work on these lines is currently under investigation for seismic soil structure interaction analysis of nuclear power plant structures.

References

Atluri, S. N. and Zhu, T. (1998): ‘A New Meshless Local Petrov-Galerkin (MLPG) Approach in Computational Mechanics’, *Computational Mechanics,* 22, pp. 117-127.

Atluri, S. N., Cho, J. Y. and Kim, H. G. (1999): ‘Analysis of Thin Beams using the Meshless Local Petrov-Galerkin Method with Generalized Moving Least Square Interpolations’, *Computational Mechanics*, 24, pp. 334-347.

Belytschko, T. and Tabbara, M. (1996): ‘Dynamic Fracture using Element-Free Galerkin Methods’, *International Journal for Numerical Methods in Engineering*, 39, pp. 923–938.

Belytschko, T., Lu, Y.Y. and Gu, L. (1994): 'Element Free Galerkin Methods', *International Journal for Numerical Methods in Engineering*, 37, pp. 229-256.

Cheung, Y. K. and Tham, L.G. (1993): 'Recent Advances in Soil-Structure Interaction Analysis', *Proc. of the Theory and Applications of the Structures Media Interaction,* Hohai University Press, Nanjing, pp. 17–27.

Dodagoudar, G. R. and Venkatachalam, G. (2000a): 'Reliability Analysis of Slopes using Fuzzy Sets Theory', *Computers and Geotechnics*, 27, pp. 101 – 115

Dodagoudar, G. R. and Venkatachalam, G. (2000b): 'Modelling of Fuzzy Information in Geotechnical Engineering', *Proc. of the Indian Geotechnical Conf., IGC-2000, The Millenium Conference*, pp. 155 – 158.

Dolbow, J. and Belytschko, T. (1998): 'An Introduction to Programming the Meshless Element-Free Galerkin Method', *Archives in Computational Mechanics*, 5, pp. 207–241.

Dong, W. and Shah, H. (1987): 'Vertex Method for Computing Functions of Fuzzy Variables', *Fuzzy Sets and Systems*, 24, pp. 65-78.

Hellendoorn, H. and Thomas, C. (1993): 'Defuzzification in Fuzzy Controllers', *Intelligent and Fuzzy Systems*, 1, pp. 109 – 123.

Hetenyi, M., (1958): *Beams on Elastic Foundation,* The University of Michigan Press, Michigan.

Kaljevic, I. and Saigal, S. (1995): 'Stochastic Boundary Elements for Two-Dimensional Potential Flow in Homogeneous Domains', *International Journal of Solids and Structures,* 32, pp. 1873-1892.

Krongauz, Y. and Belytschko, T. (1996): 'Enforcement of Essential Boundary Conditions in Meshless Approximation using Finite Elements', *Computer Methods in Applied Mechanics and Engineering*, 131, pp. 1335–1345.

Liu, G. R. (2003): *Mesh Free Methods: Moving Beyond the Finite Element Method*, CRC Press, Boca Raton.

Liu, G. R. and Gu, Y. T. (2000): 'Coupling of Element Free Galerkin Method and Hybrid Boundary Element Methods using Modified Variational Formulation', *Computational Mechanics,* 26, pp. 166 -173.

Lu, Y. Y., Belytschko, T. and Gu, L. (1994): 'A New Implementation of the Element Free Galerkin Method', *Computer Methods in Applied Mechanics and Engineering*, 113, pp. 397–414.

Lu, Y. Y., Belytschko, T. and Tabbara, M. (1995): 'Element Free Galerkin Methods for Wave Propagation and Dynamic Fracture', *Computer Methods in Applied Mechanics and Engineering*, 126, pp. 131–153.

Nayroles, B., Touzot, G. and Villon, P. (1992): 'Generalizing the Finite Element Method: Diffuse Approximation and Diffuse Elements', *Computational Mechanics,* 10, pp. 307-318.

Rao, B. N. and Rahman, S. (2000): 'An Efficient Meshless Method for Fracture Analysis of Cracks', *Computational Mechanics*, 26, pp. 398-408.

Shepard, D. (1968): 'A Two-Dimensional Function for Irregularly Spaced Data', *Proc. of ACM National Conference,* pp. 517-524.

Sukumar, N., Moran, B., Semenov, A. Y. And Belikov, V. V. (2001): 'Natural Neighbour Galerkin Methods', *International Journal for Numerical Methods in Engineering*, 50, pp. 1 - 27.

Sunitha, N. V. (2007): *Fuzzy Finite Element and Meshless Methods for Soil Structure Interaction Problems*, M. S. Thesis, I I T Madras, Chennai.

Zadeh, L. A. (1965): 'Fuzzy Sets', *Information and Control*, 8, pp. 338 - 353.

Zadeh, L. A. (1978): 'Fuzzy Sets as a Basis for a Theory of Possibility', *Fuzzy Sets and* , 1, pp. 3-28.